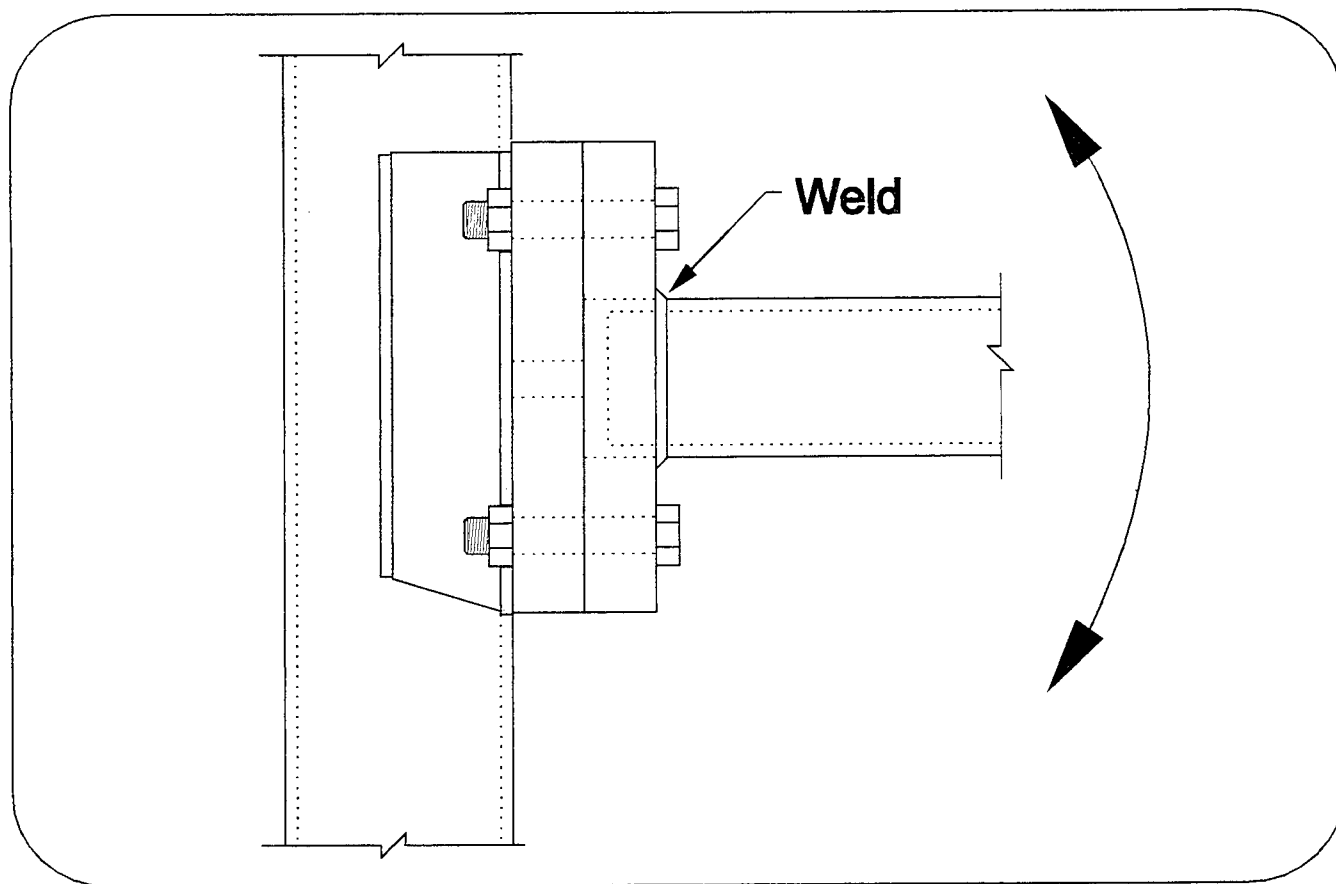


Fatigue of Tube-to-Plate Fillet Welds and Methods for Their Improvement



PB98-125628




Physical Research Report No. 118
July 1997



Illinois Department of Transportation
Bureau of Materials and Physical Research

REPRODUCED BY:
U.S. Department of Commerce
National Technical Information Service
Springfield, Virginia 22161

NTIS

1. Report No. FHWA/IL/PR-118	2. Government Accession No.	3.  PB98-125628
4. Title and Subtitle FATIGUE OF TUBE-TO-PLATE FILLET WELDS AND METHODS FOR THEIR IMPROVEMENT	5. report date July 1997	6. Performing Organization Code
7. Author(s) Jeffrey M. South, PE	8. Performing Organization Report No. PRR-118	10. Work Unit (TRAIS)
9. Performing Organization Name and Address Illinois Department of Transportation Bureau of Materials and Physical Research 126 E. Ash St. Springfield, IL 62704-4766	11. Contract or Grant No. IHR-319	13. Type of Report and Period Covered Final Report January 1994 through April 1996
12. Sponsoring Agency Name and Address Same	14. Sponsoring Agency Code	
15. Supplementary Notes Study conducted in cooperation with the U.S. Department of Transportation, Federal Highway Administration.		
16. Abstract This report documents fatigue testing of tube-to-plate fillet welds. Twenty-four specimens were tested at six stress ranges in order to develop a fatigue relationship between nominal stress range (S) and cycles to failure (N) for this common weld detail. The data agree with the limited data found in the literature for similar details. The data from this study were combined with literature data to develop a reasonable composite N-S equation for use in design. The composite N-S equation is $N = 8.79 \times 10^8 [S]^{-3.43}$ (with S in ksi) and represents 95 percent confidence/95 percent probability limits. The equation estimates fatigue strengths of 5.9 and 3.7 ksi (41 and 26 MPa) at two and ten million cycles, respectively, for a tube-to-plate fillet weld with loose fit-up and no tube-to-plate end bearing contact. Several methods for improving the fatigue strength of welded connections, including grinding, tungsten-inert gas (TIG) dressing, and peening were evaluated. To improve performance the weld toe should be lightly ground to a depth of about 0.01 inch (0.3mm) and the entire weld should be peened prior to galvanizing. Preheat of the connection components is also recommended.		
17. Key Words Fatigue, testing, tube-to-plate fillet welds, grinding, TIG dressing, peening, improved performance.	18. Distribution Statement No restrictions. This document is available to the public through the National Technical Information Service, Springfield, Virginia 22161.	
19. Security Classif. (of this report) Unclassified	20. Security Classif. (of this page) Unclassified	21. No. of Pages 43
		22. Price

FATIGUE
OF
TUBE-TO-PLATE FILLET WELDS
AND
METHODS FOR THEIR IMPROVEMENT

Jeffrey M. South, PE
Engineer of Technical Services

Physical Research Report No. 118
Illinois Department of Transportation
Bureau of Materials and Physical Research
Springfield, Illinois
July 1997

Table of Contents

<u>Foreword</u>	i
<u>Notice</u>	i
<u>Acknowledgments</u>	i
<u>List of Figures</u>	ii
<u>List of Tables</u>	ii
I. Introduction	1
II. Experimental Procedures	3
<u>Test Apparatus</u>	3
<u>Instrumentation</u>	3
<u>Specimens</u>	4
<u>Test Conditions</u>	4
<u>Definition of Failure</u>	12
<u>Determination of Stress Concentration Factor, K_t</u>	13
III. Experimental Results	14
<u>Results of Previous Research</u>	14
<u>Data Collected</u>	18
IV. Methods to Improve Weld Fatigue Life	24
<u>Background</u>	24
<u>Grinding</u>	24
<u>Weld Toe Dressing</u>	25
<u>Peening</u>	27
<u>Closure</u>	29
V. Summary	31
VI. Conclusions and Recommendations	33
References	35
Appendix: Determination of Confidence And Probability Limits	36

Foreword

This report should be of interest to engineers involved in structural design, planning, maintenance and inspection; consultants; and other technical personnel concerned with the fatigue life of structures.

Notice

The contents of this report reflect the views of the author who is responsible for the facts and the accuracy of the data presented herein. The contents do not necessarily reflect the official views or policy of the Federal Highway Administration or the Illinois Department of Transportation. This report does not constitute a standard, specification, or regulation.

Neither the United States Government nor the State of Illinois endorses products or manufacturers. Trade or manufacturers' names appear herein solely because they are considered essential to the object of this report.

Acknowledgments

The author gratefully acknowledges the kind assistance and support of Mr. Christopher Hahin, Engineer of Bridge Investigations; and Messrs. Tom Courtney, Russ Gotschall, Harry Smith, and Ken Wyatt of the Illinois Department of Transportation.

List of Figures

<u>Figure No.</u>	<u>Description</u>	<u>Page</u>
1	Photograph of the test apparatus.	5
2	Mechanism used for specimen tip deflection.	6
3	Close-up photograph of adjustable cam.	7
4	Close-up photograph of typical specimen instrumentation.	8
5	Photograph of a complete specimen failure.	9
6	Drawing of test specimen showing pertinent dimensions.	10
7	Schematic diagram of fully reversed cyclic loading with zero mean stress used in this study.	11
8	Weld details used by Archer and Gurney. (a) is their Type F specimen, (b) is Type S.	15
9	Data of study from Archer and Gurney.	17
10	Data collected in the current study.	19
11	Data from this investigation combined with the Type S specimen data of Archer and Gurney.	22
12	(a) Recommended method of disc grinding. (b) Recommended method of burr grinding. Recommendations made by Booth [Ref. 7].	26

List of Tables

<u>Table No.</u>	<u>Description</u>	<u>Page</u>
1	Fatigue Strengths of Various AWS Tubular Weld Categories	2
2	Applied Strain Ranges Used For Fatigue Testing	12
3	Fatigue Data for Mild Steel Fillet Welded Tube-to-Plate Joints	16
4	Cycles to Failure for Fillet Welded Tube-to-Plate Connection	18
5	Fatigue Strength Improvement of Peened Non-Load-Carrying Fillet Welds	28

I. INTRODUCTION

This document is the final report for Research Project IHR-319 "Fatigue of Overhead Sign and Signal Structures." The research study was started in response to wind-related fatigue failures of some sign and signal structures in Illinois and other states. Low fatigue life of tube connections in sign and signal structures is a possible cause of failure. This investigation was undertaken because of the effect of structure failures on public safety. Prior work for IHR-319 concerned (a) methods to estimate forces due to vortex shedding; (b) acquisition of wind speed data and stress range-frequency histograms of details subjected to ambient wind loads; (c) cumulative damage evaluation using previously published fatigue life equations; and (d) calculation of a factor of safety for various weld details. That work was published in May 1994 as Physical Research Report 115, "Fatigue Analysis of Overhead Sign and Signal Structures" [Ref. 1]. The current report determines the fatigue strength and presents equations relating applied stress range to expected number of cycles-to-failure for a tube-to-plate weld not addressed by current codes.

To predict fatigue damage to a weld with reasonable accuracy, one must be able to determine the available number of cycles to failure at a given stress range. The American Welding Society (AWS) publishes conservative stress range versus number of cycles to failure (S-N) diagrams for weld categories [Ref. 2, p. 167] from which equations relating applied stress range to available cycles to failure were developed by South [Ref. 1] for tube welds and Hahin *et al.* [Ref. 3] for plate welds. Traditional S-N equations are of the form $N=C[S]^m$ where S is the applied stress range, N is the expected number of cycles to failure, and C and m are the intercept and slope of the data regression line, respectively.

Some AWS weld categories have extremely low fatigue strengths, as seen in Table 1. One of the most common welds in overhead sign and signal structures is a circumferential tube-to-plate fillet weld. This connection is not specifically addressed by the AWS fatigue categories. Based on AWS data, the allowable stress range for the closest similar weld (Category ET) is about 2 ksi (14 MPa) at ten million cycles. This stress range is very low compared to unwelded tube (Category A) and indicates that Category ET welds are very susceptible to fatigue damage. Fatigue testing of tube-to-plate fillet weld connections was needed to evaluate the fatigue susceptibility of this weld type found in many sign and signal structures. These results are also applicable to other common industrial or public works structures.

The purposes of this study were to develop nominal stress range versus cycles to failure data for tube-to-plate circumferential fillet welds in the as-welded condition and to examine treatment methods to improve their fatigue resistance. This data will then be available for

fatigue analysis of these particular weld connections, and for comparison with published fatigue data. Fatigue strength of tube-to-plate welds is typically reported at two and ten million cycles. The stress range vs. available cycles-to-failure equations presented are appropriate for design purposes.

TABLE 1

Fatigue Strengths of Various AWS Tubular Weld Categories

<u>Weld Category</u>	Fatigue Strength (ksi)	
	<u>2x10⁶ Cycles</u>	<u>10⁷ Cycles</u>
A	25	25
B	17	14
C ₁ and X ₁	16	9.8
F	10	8.3
C ₂ and X ₂	11	7.5
D	9	5.5
FT	5	4
DT	6	4.2
E	8	4.5
K ₁	2.2	1.5
ET	3	1.9
K ₂	1.8	1.3

Data Source: Figure 10.7.4, AWS D1.1-84.
To convert ksi to MPa, multiply by 6.895.

II. EXPERIMENTAL PROCEDURES

The purpose of this chapter is to discuss the experimental procedures used in this study including test apparatus, instrumentation, specimens, and test conditions.

Test Apparatus

Various photographs of the test apparatus are shown in Figures 1 through 3. The test device is basically a stout platform for mounting specimens in a convenient configuration for repeated load application. The method of load application is through cantilever bending by vertical deflection of each specimen tip.

Figure 1 shows an overall view of the test apparatus. An electric motor and speed reducer operate the central driveshaft that extends longitudinally between the two horizontal steel beams. Each specimen is deflected by an adjustable cam and slider-crank mechanism as shown in Figures 2 and 3. The apparatus is configured so that specimens on the opposite sides of the central post are deflected in the same direction at the same time (i.e. deflections are in phase). Side-by-side specimens are not necessarily in phase because the two sets of mounts are structurally independent. Specimens are bolted to the uprights by threaded rods which extend through the upright. The attachment method resembles that commonly used to connect traffic signal mast arms to vertical standards.

Instrumentation

Two types of instrumentation were used for the experiments. Crack detector gages (Type DC-02-15A, MicroMeasurements, Inc., Raleigh, NC) were attached to detect cracks and stop testing by opening relay switches that cut power to the motor. Cycles were accumulated by a counter and magnetic switch. These gages were not used after the first test set because of problems with bonding them across the weld surface.

Strain gages (Type CEA-06-032-UW-120, MicroMeasurements, Inc., Raleigh, NC) were bonded typically 1/32 inch [0.8 mm] from the weld toe at a point of maximum bending stress (twelve o'clock looking at a cross section). This gage has a sensing grid 1/32 inch (0.8 mm) long. The strain gages were used to set the specimen tip deflection for a given test condition as discussed later. The strain gages were connected to a data acquisition system (Model 2100, Somat Corp., Champaign, IL) which counted cycles and monitored applied strain ranges using the internal rainflow cycle counting algorithm. The actual strain measured included some level of stress concentration because of the proximity of the strain gage to the weld toe.

The stress concentration at the gage location was measured to be 1.78. The procedure used to determine the stress concentration is described later in this chapter. A typical strain gage/crack detector installation is shown in Figure 4. A typical specimen failure is shown in Figure 5.

Specimens

The specimens used for this study were fabricated from 3 inch (76 mm) outer diameter, 1/8 inch (3.2 mm) wall thickness, AISI 1020 drawn-over-mandrel (DOM) steel tube and 1 inch (25.4 mm) thick ASTM A36 steel plate. The components were connected by a 1/4 inch (6.4 mm) circumferential fillet weld. The ratio of weld leg to tube wall thickness was 2.0. The weld electrode used was AWS E7018. The tube tip to weld toe length is approximately 6 feet (1.8 m). Pertinent specimen dimensions are shown in Figure 6. The specimens were tested in the as-welded condition.

Test Conditions

Fatigue testing was conducted at the Physical Research Laboratory in Springfield, Illinois. The facility is heated and able to maintain a reasonably constant room temperature near 70°F.

Strain was used as the independent variable for this study because measured strains tend to be more accurate than calculated stresses, especially near a discontinuity like a weld. The specimen loading situation for this study was fully reversed cyclic loading with zero mean strain, shown schematically in Figure 7. The frequency of loading was three cycles per second (3 Hz) where a cycle is defined as shown in Figure 7. Six applied strain ranges were used in the experiments as shown in Table 2. The strain range is defined as:

$$\Delta\varepsilon = \varepsilon_{\max} - \varepsilon_{\min} \quad (1)$$

where $\Delta\varepsilon$ = strain range,
 ε_{\max} = maximum strain, and
 ε_{\min} = minimum strain.

Four specimens were tested at each strain range.

The deflection amplitudes for the specimen groups were set by using the strain gages to measure the strain near the weld for an applied tip deflection. The following procedure was used to set the tube tip deflections:

1. The strain gage circuit was balanced and zeroed.
2. The linkage was attached to the tube tip.

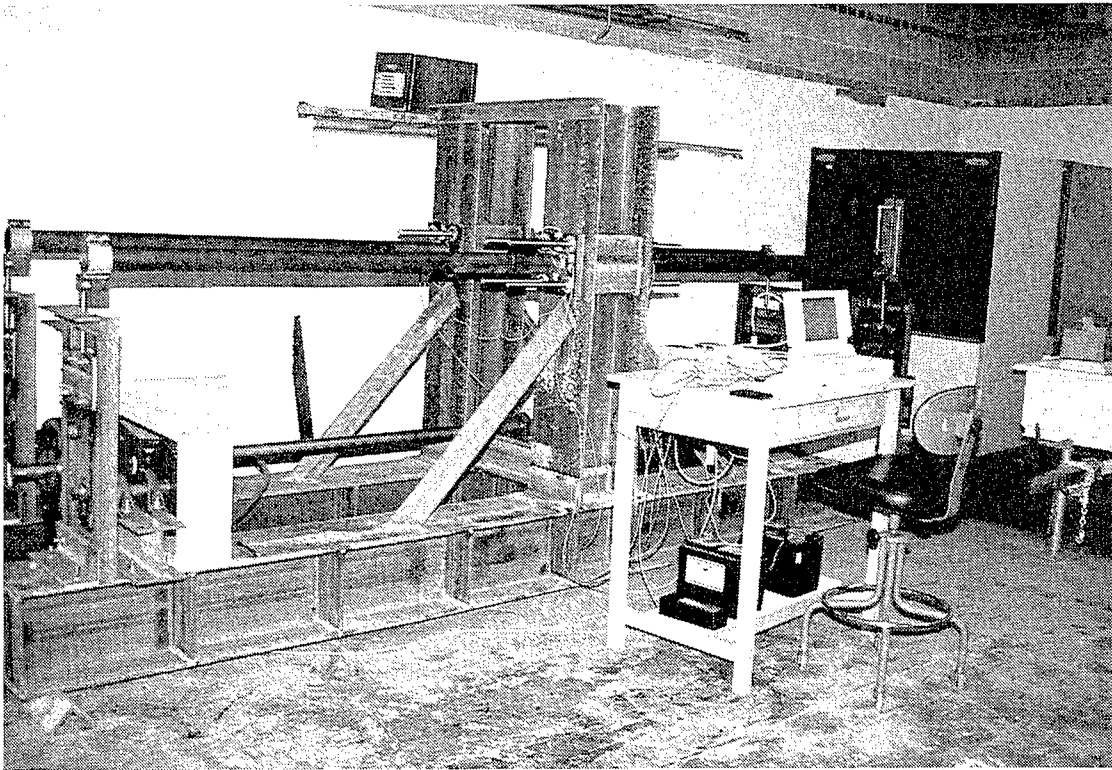


Figure 1. Photograph of the test apparatus. Electric motor rests between horizontal beams and is seen on left side of apparatus. Note the simultaneous (in phase) deflection of the specimens on either side of the vertical connection beam. Side-by-side specimens are also coincidentally in phase. Data acquisition system is on the work table.

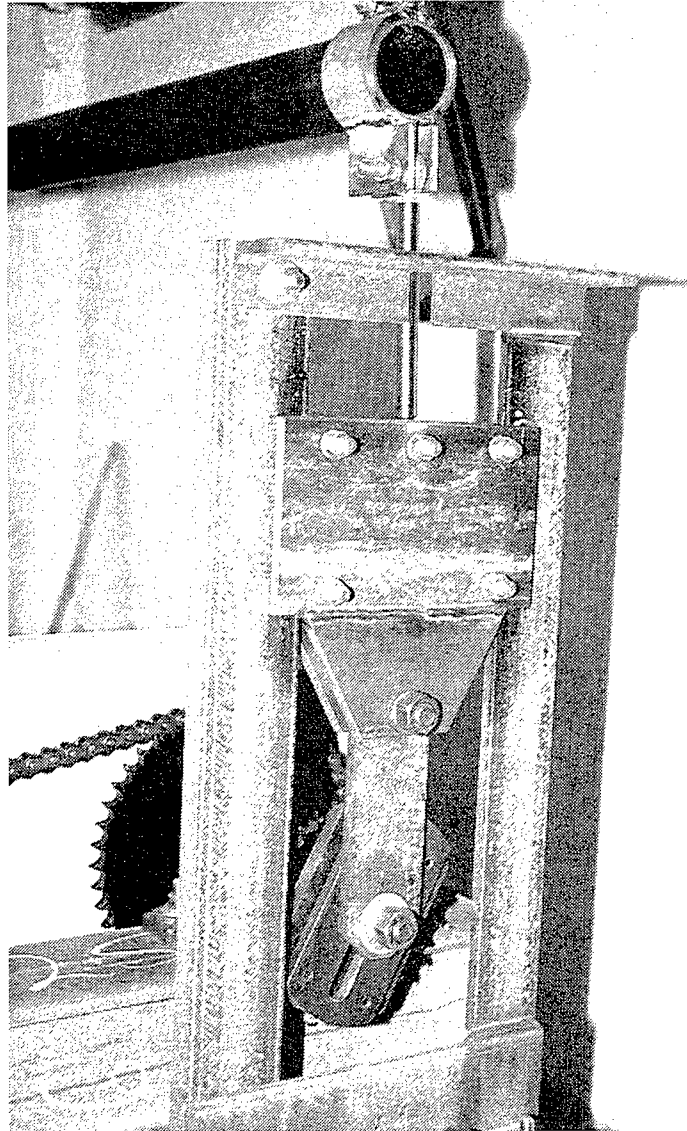


Figure 2. Mechanism used for specimen tip deflection. Sprocket in back is driven from speed reducer. Cam at bottom of mechanism is variable. Vertical slide and interior rollers were kept well-lubricated. Upper link extends from specimen tip down to top of slide mechanism.

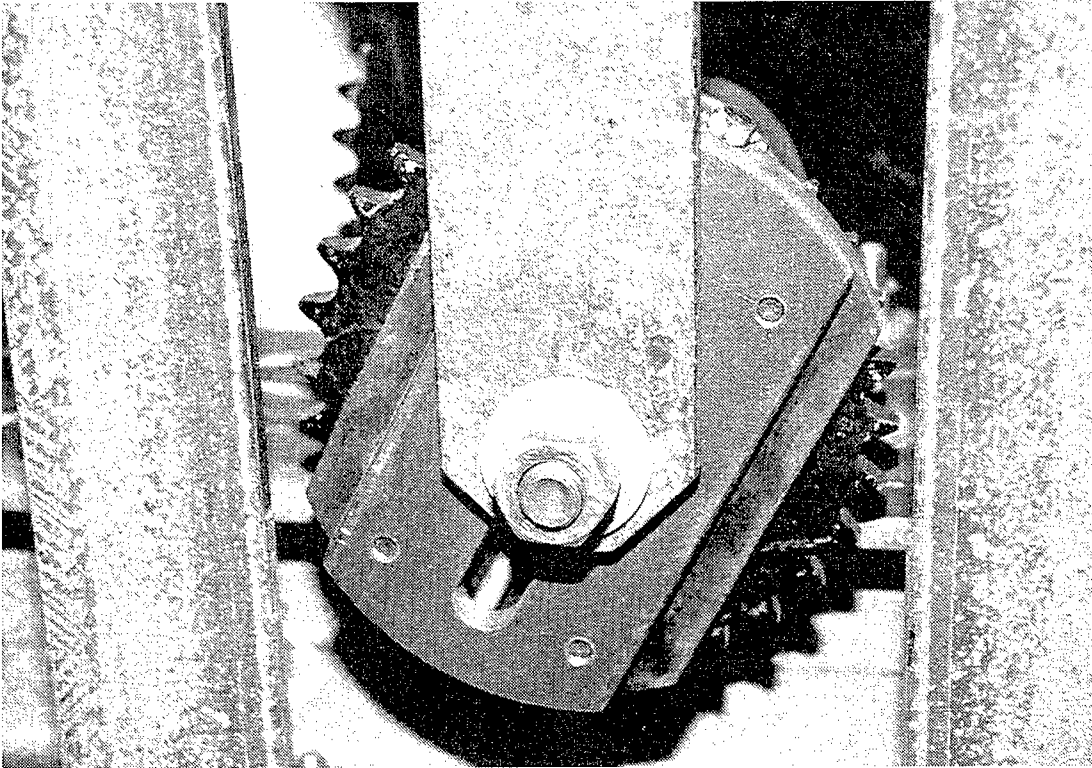


Figure 3. Close-up photograph of adjustable cam. Lower link is attached to cam and extends up to the slide mechanism (shown in Figure 2).

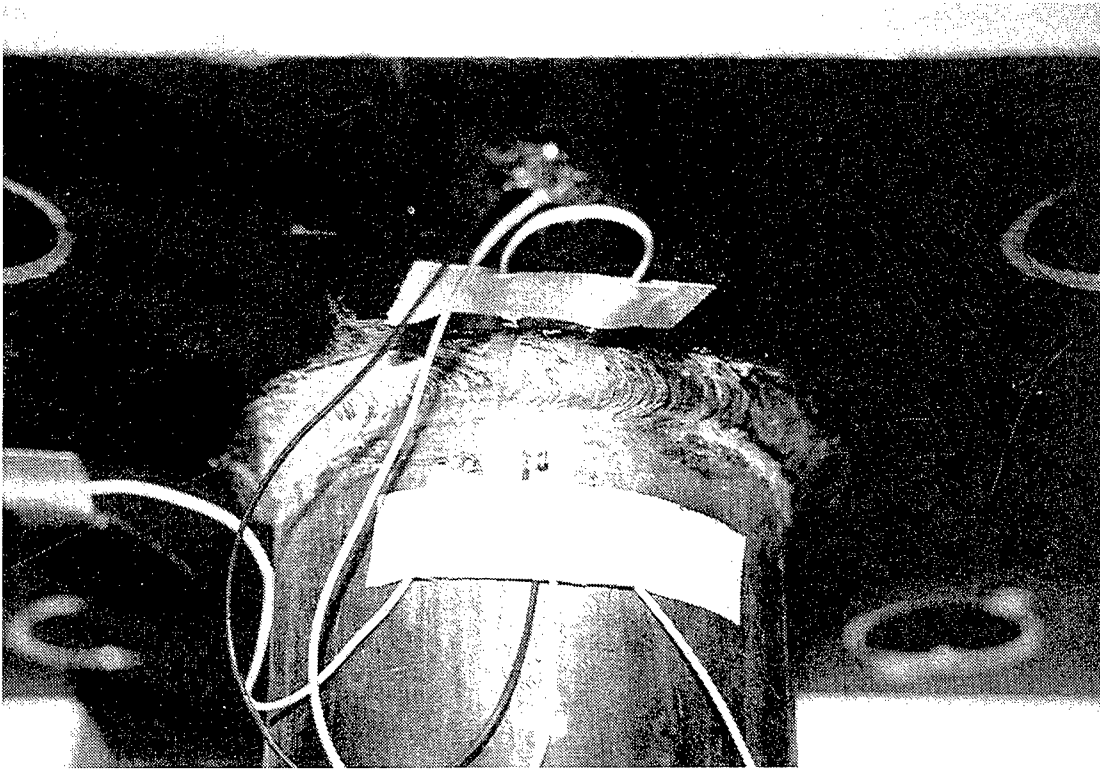


Figure 4. Close-up photograph of typical specimen instrumentation. Crack detection gages extend over the entire weld and onto the tube. Strain gage is as close to the weld as possible.

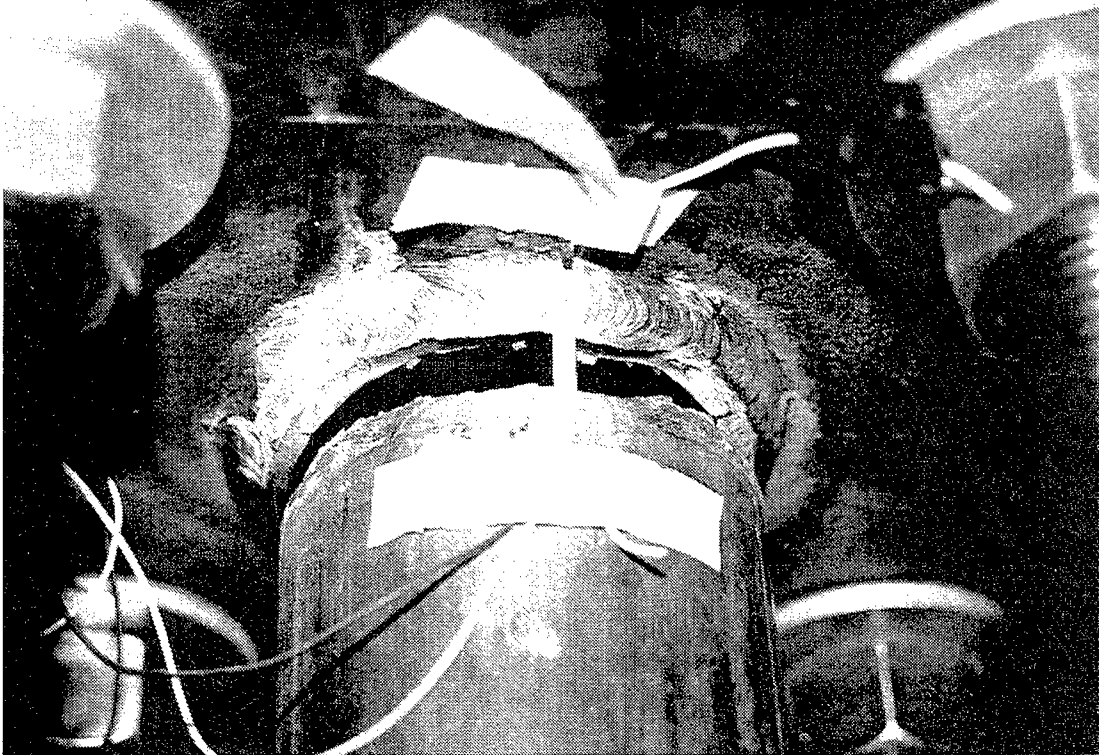


Figure 5. Photograph of a complete specimen failure. Note that one crack detector broke (cycle data collection was suspended at that time) and the other debonded without rupturing. Note also the occurrence of failure at the weld toe. This failure location was consistent for all failures.

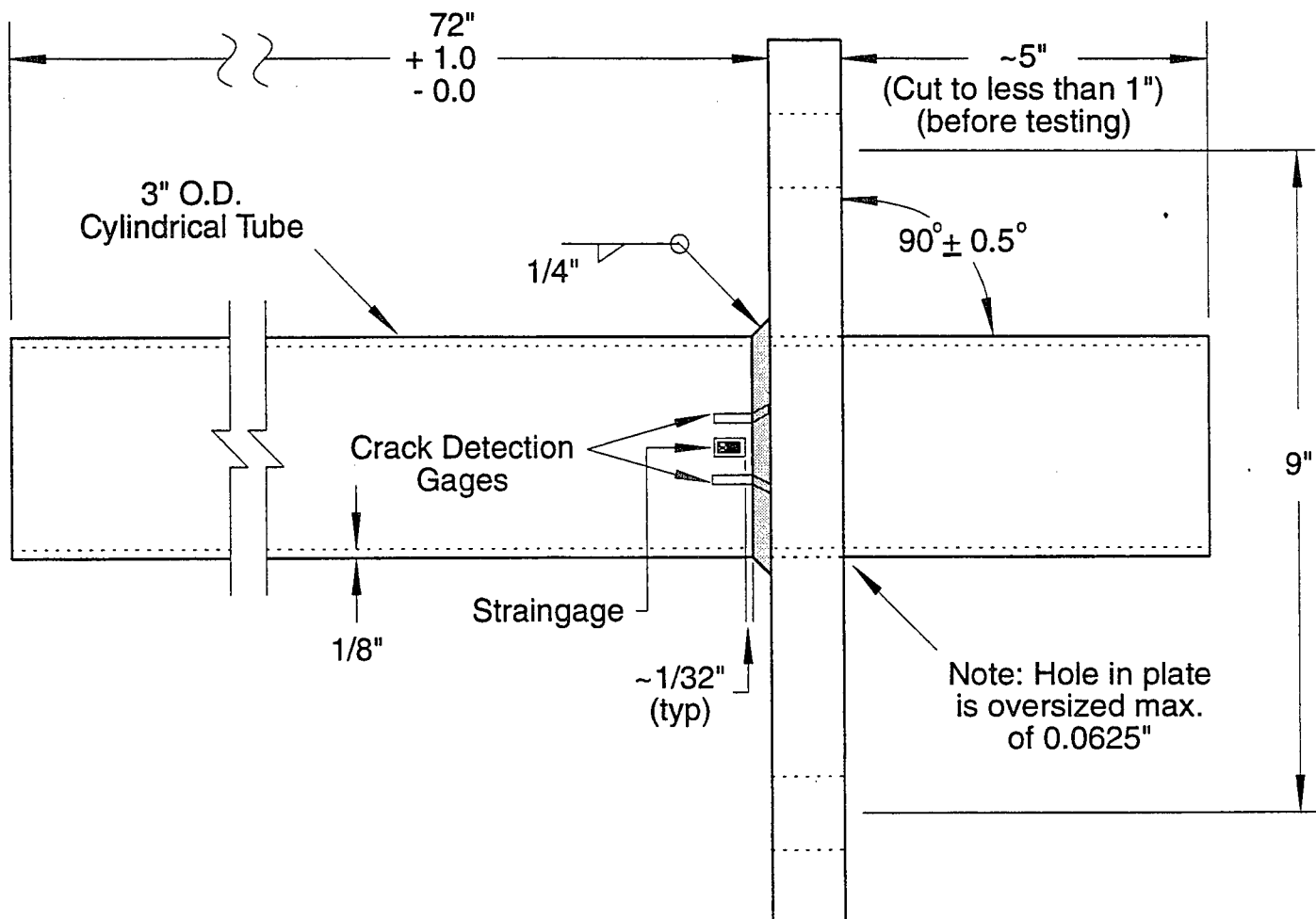


Figure 6. Drawing of test specimen showing pertinent dimensions. View is from above. Drawing is not to scale.

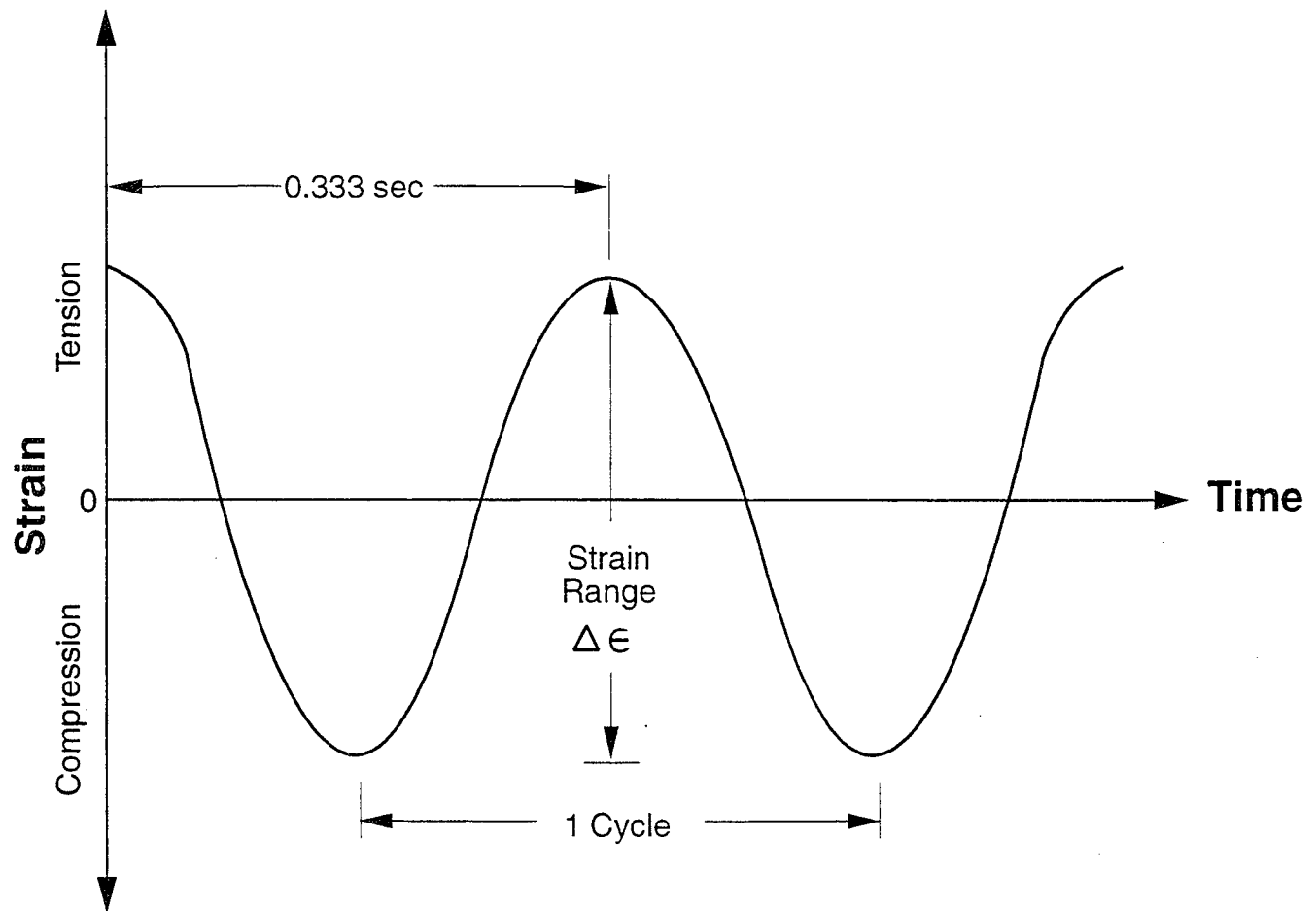


Figure 7. Schematic diagram of fully reversed cyclic loading with zero mean strain used in this study.

3. The linkage was rotated to the full down position.
4. The cam was adjusted to get the desired tensile strain reading.
5. The linkage was rotated to the full up position.
6. The upper link on the slide mechanism was adjusted to get the desired compressive strain.

Steps 3-6 were repeated until the proper strain range was obtained. The upper link of the slide mechanism had to be adjustable since the tube tip at zero strain did not necessarily have the same position from specimen to specimen.

TABLE 2

Applied Strain Ranges Used For Fatigue Testing

Strain Range, $\Delta\epsilon$ (<u>Microstrain</u>)	Corresponding Nominal Stress Range, S^* (<u>ksi</u>)
500	8.4
667	11.2
1000	16.9
1167	19.7
1333	22.5
2000	33.7

* $S = E\Delta\epsilon/K_t$, where $E = 30 \times 10^6$ psi, stress concentration $K_t = 1.78$.
To convert ksi to MPa, multiply values by 6.895.

Definition of Failure

The detection of the onset of failure used for this study was that crack initiation occurred when the strain gage instrumentation began recording both nonzero mean strains and strain range events outside of the range originally set by deflection. A change in both parameters would imply that a measureable change had occurred that was not related to zero shift in the instrumentation. For the load method used, crack initiation near the gage caused the tensile portion of the cycle to be reduced. This caused the total measured strain range to change. The ratio of minimum to maximum strain, called the strain ratio, changed (became more negative) from the initial value of -1. Crack initiation 180 degrees from the gage caused the compressive part of the cycle to change and caused the strain ratio to become less negative. The welds were visually checked for cracks when the criteria were met. Visible cracks always

correlated with the above criteria. The cycle counting algorithm used by the data acquisition system was able to record small changes in the measured strain conditions.

Determination of Stress Concentration Factor, K_t

An experiment was conducted to determine the apparent stress concentration at the location of the strain gage. This was necessary because of the proximity of the strain gage to the weld toe. The experiment included measuring the strain at the strain gage due to a measured tip deflection and then calculating the expected nominal strain due to the same deflection using normal analytical techniques. The ratio of measured strain to calculated strain is the stress concentration factor K_t (assuming elastic behavior). The average measured value of K_t was 1.78. The standard deviation of the data was 0.014. Sixteen measurements were taken.

The applied strain ranges used during testing were reduced (divided) by K_t to report the data in terms of the nominal stress range calculated by simple bending theory. This experiment did not measure the actual stress concentration at the weld toe since the center of the strain gage grid was approximately 3/64 inch (1.2 mm) away from the toe.

III. EXPERIMENTAL RESULTS

The purpose of this chapter is to present and discuss the data collected during the course of this study. The data are used to estimate fatigue strength at two and ten million cycles and to develop a stress-life equation modified for high cycle fatigue. This research augments previously published work on fatigue of tube-to-plate fillet welds.

Results of Previous Research

Published data on fatigue strength of fillet-welded tube-to-plate joints for mild steel is very limited. Archer and Gurney [Ref. 4] tested two joint configurations:

1. Tubes fillet welded directly to plate (specimen Type F).
2. Tubes inset into a thick sleeve and fillet welded (specimen Type S).

The Type F joints, shown in Figure 8a, consisted of a 5.5 inch (139.7 mm) diameter plate with a length of 4.5 inch (114.3 mm) outer diameter tube welded to each side. Tube wall thickness was 0.5 inch (12.7 mm). To ensure coaxiality the plate was machined on each side to leave a short locating spigot. The tubes were bored for a short distance to ensure good fit over the spigot. Three fillet weld sizes were investigated, 5/16 inch (7.9 mm), 7/16 inch (11.1 mm), and 11/16 inch (17.5 mm).

The Type S joint, shown in Figure 8b, consisted of a 6 inch (152.4 mm) outer diameter, 3 inch (76.2 mm) long sleeve whose inside diameter was 1/8 inch (3.2 mm) greater than that of the insert tube. According to Archer and Gurney, this clearance gave a fit-up comparable to that used in practice. Sleeve wall thickness was not given, but appears to be about 1 inch (25.4 mm) based on the given drawing. Weld sizes were 7/16 inch (11.1 mm) and 9/16 inch (14.3 mm). The test method used was rotating bending. Welds and fit-up used in the current study resembled the Type S specimens.

Table 3 and Figure 9 show Archer and Gurney's data for weld toe failures. The data were converted in the current study from their units of tonf/in^2 ($1 \text{ tonf/in}^2 = 15.4 \text{ N/mm}^2$) to ksi ($1 \text{ tonf/in}^2 = 2.2 \text{ ksi}$) for comparison purposes. Also, for example, the notation ± 5 was interpreted as a range of 10.

Archer and Gurney reported mean fatigue strengths of 15 ksi (103 MPa) at two million cycles for Type F details and 12.1 ksi (83 MPa) for Type S details. A regression analysis of their data was made for the current study using failures in the weld toe only. Weld toe failures were used for this analysis because modern welds are sized in design to preclude throat failures.

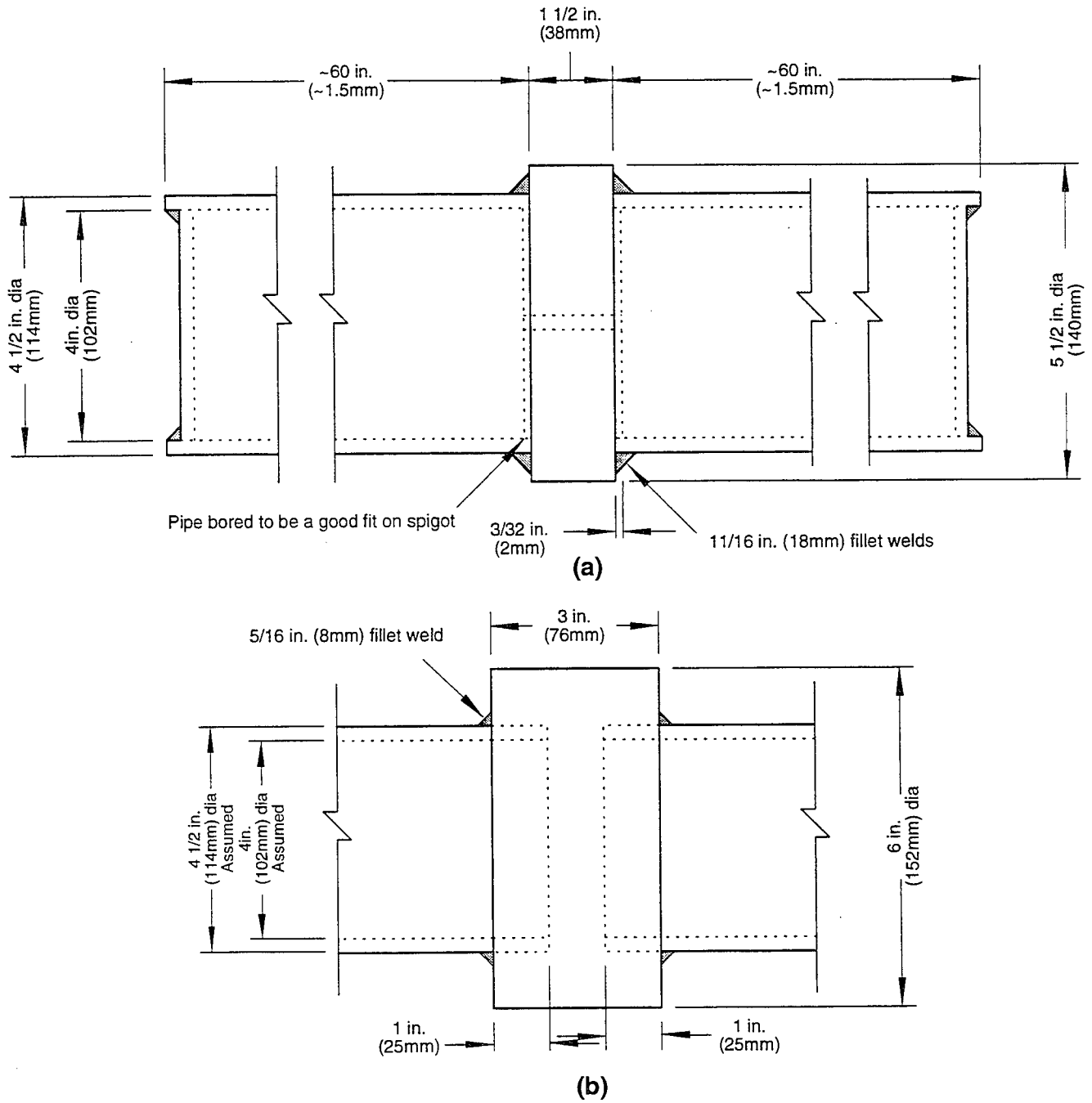


Figure 8. Weld details used by Archer and Gurney. (a) is their Type F specimen, (b) is Type S. Tube dimensions for their Type S specimens are assumed to be the same as those of the Type F specimens. Loading was in rotating bending.

Table 3
Fatigue Data for Mild Steel Fillet Welded Tube-to-Plate Joints
Archer and Gurney
(Failure in Weld Toe Only)

Type F Specimens

<u>Stress Range (ksi)</u>	<u>Cycles to Failure</u>
24.2	8.0×10^5
22	8.1×10^5
19.8	1.3×10^6
17.6	1.2×10^6
15.4	1.9×10^6
15.4	2.0×10^6

All 11/16 inch (17.5 mm) fillet welds.

Type S Specimens

<u>Stress Range (ksi)</u>	<u>Cycles to Failure</u>
24.2	3.1×10^5 (1)
22	3.5×10^5 (2)
17.6	5.5×10^5 (1)
15.4	4.3×10^5 (1)
14.3	8.0×10^5 (2)
13.2	2.4×10^6 (1)

Notes: (1): 9/16 inch (14.3 mm) fillet welds.

(2): 7/16 inch (11.1 mm) fillet welds.

To convert ksi to MPa, multiply values by 6.895.

Data source: Archer, G.L. and Gurney, T.R., Fatigue Strength of Mild Steel Fillet Welded Tube to Plate Joints, *Metal Construction*, Volume 2, Number 5, 1970, pp. 207-210.

The analysis provided the following equations for Type F details:

$$S = 1.97 \times 10^4 [N]^{-0.495} \quad \text{or} \quad (2a)$$

$$N = 4.7 \times 10^8 [S]^{-2.019} \quad (r^2 = 0.91, \text{ Standard Error of Estimate [SEE] = 1.15}) \quad (2b)$$

The following equations are for Type S details:

$$S = 3.34 \times 10^3 [N]^{-0.395} \quad \text{or} \quad (3a)$$

$$N = 8.34 \times 10^8 [S]^{-2.533} \quad (r^2 = 0.66, \text{ SEE} = 1.63) \quad (3b)$$

Stress range S is in ksi. The higher fatigue strength and the better curve fit for the Type F specimens are a consequence of the tighter fit-up used in making the specimens and the fact that the end of the tube butted the plate to which it was welded. The bearing contact would tend to improve fatigue performance of the weld. The looser fit-up of the Type S specimens and lack of bearing contact from the thick sleeve contributed to reduced fatigue strength and the poorer curve fit. These equations are also plotted on Figure 9.

Figure 9. Data from study by Archer and Gurney [Ref. 4]. Data are failures in the weld toe. Type F specimens were machined to fit over a spigot on the plate. The end of the tube had bearing contact on the plate. The mean regression equation for the Type F data is $S=1.97 \times 10^4 [N]^{-0.495}$ with $r^2=0.91$. Mean fatigue strength at 2×10^6 cycles is 15 ksi (103 MPa). Mean fatigue strength at 10^7 cycles is estimated to be 6.8 ksi (47 MPa). Type S specimen tubes were inserted into a thick sleeve with loose fit-up and then welded. The end of the tube did not bear on a surface. The mean regression equation for the Type S data is $S=3.34 \times 10^3 [N]^{-0.395}$ with $r^2=0.66$. Mean fatigue strength at 2×10^6 cycles is 10.8 ksi (75 MPa). Mean fatigue strength at 10^7 cycles is estimated to be 5.7 ksi (39 MPa). The Type S specimens resemble the welds tested in the current study in terms of fit-up and lack of bearing contact.

In the Type F series, weld toe failures occurred only in the specimens with 11/16 inch (17.5 mm) welds. Weld toe failures occurred in both the 7/16 inch (11.1 mm) and the 9/16 inch (14.3 mm) welds in the Type S series, although there were also some weld root failures in the 7/16 inch (11.1 mm) specimens. The number of specimens tested at each stress level is unknown. The test setup (opposing tubes in rotating bending) implies that at least two welds were tested at each stress level. Archer and Gurney did not discuss the variability of their data.

A significant body of data exists for tube-to-tube welds and is summarized by Gurney [Ref. 5, Ch. 7]. This type of tubular connection is in fact the type specifically referred to in the AWS structural welding code [Ref. 1, p. 230]. Number of cycles to failure (N) versus stress range (S) equations are published for these various weld categories [Ref. 1, pp.79-81].

Data Collected

The data collected in this study are given below in Table 4. Nominal stress range was determined from $S = E\Delta\epsilon/K_t$ where $E = 30 \times 10^6$ psi and $K_t = 1.78$. Nominal stress range versus cycles to failure is also graphed in Figure 10.

Table 4
Cycles to Failure for Fillet-Welded Tube-to-Plate Connection

	Nominal Stress Range (ksi)					
	33.7	22.5	19.7	16.9	11.2	8.4
Specimen 1	62,565	216,372	581,212	299,657	$>1.5 \times 10^{7*}$	10,416,673*
Specimen 2	157,804	213,422	570,601	2,568,000	$>1.5 \times 10^{7*}$	10,416,673*
Specimen 3	35,629	291,300	199,694	1,322,214	$>1.5 \times 10^{7*}$	10,416,673*
Specimen 4	40,819	182,166	581,206	1,181,967	$>1.5 \times 10^{7*}$	6,243,700
Mean	74,204	225,815	483,178	1,342,960	-	-
Std. Dev.	49,312	40,113	163,727	808,634	-	-

* Testing stopped without failure.

The data in Table 4 above show no failures for the 11.2 ksi test set, and one failure for the 8.4 ksi test set. The apparent discrepancy is attributed to variability in the welding process which can produce variations in fillet geometry, weld toe undercut, slag inclusions, and porosity. A similar occurrence is noted in the data of Archer and Gurney for the Type F specimens. The

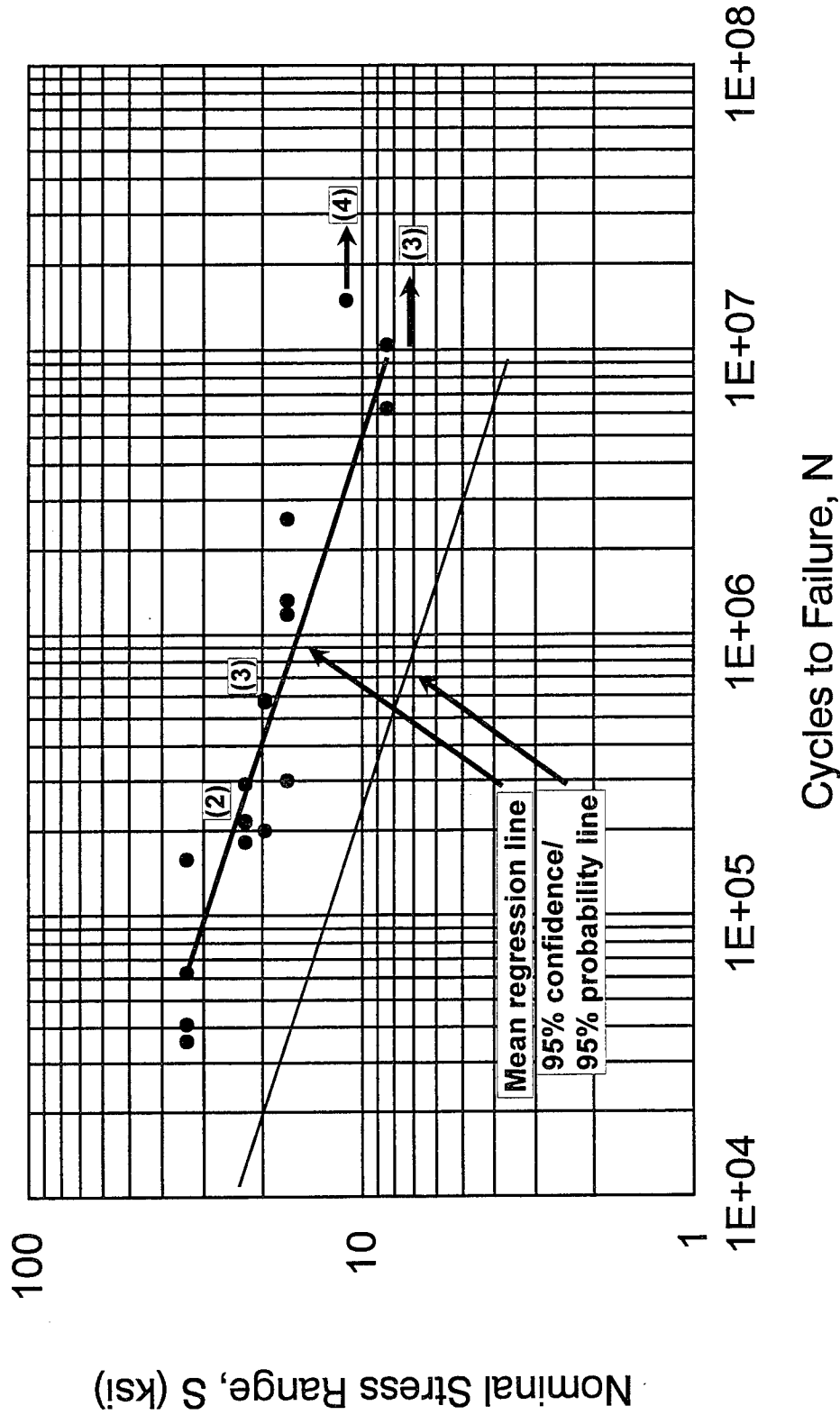


Figure 10. Data collected in the current study. Six stress ranges were used with four specimens tested at each stress range. Arrows indicate that tests ended without failure. Numbers in parentheses indicate overlapping data points. The thicker line is the mean regression equation $S=718[N]^{-0.2772}$ with $r^2=0.82$. Mean fatigue strength at 2×10^6 cycles is 12.9 ksi (89 MPa). Mean fatigue strength at 10^7 cycles is 8.2 ksi (57 MPa). The thinner line is the 95 percent confidence/95 percent probability equation $S=311[N]^{-0.2772}$. With at least 95 percent confidence, one expects at least 95 percent of all future fatigue failures for tube-to-plate welds with similar fit-up tolerances in the as-welded condition to be above this line. Fatigue strengths for this equation are 5.6 ksi (39 MPa) at 2×10^6 cycles and 3.6 ksi (25 MPa) at 10^7 cycles.

8.4 ksi failure was used in the subsequent data analysis. The 33.7 ksi data set represents a stress range of about 60 ksi as sensed by the strain gage. However, since tests were conducted using fully reversed bending with zero mean strain, this corresponds to about 30 ksi tension and 30 ksi compression. The tensile portion of the strain range is below the yield strain of AISI 1020 steel. The scatter of the data ranges from a fairly high coefficient of variation (c.o.v.) greater than 0.6 at the 33.7 and 16.9 ksi data sets, to a fairly low c.o.v of 0.18 for the 22.5 ksi data set.

A regression line was developed for the data using the method of least squares. The resulting equation is:

$$S = 718 [N]^{-0.2772} \quad \text{or} \quad (4a)$$

$$N = 2.042 \times 10^{10} [S]^{-3.608} \quad (r^2 = 0.82, \text{SEE} = 1.83) \quad (4b)$$

For stress range S in ksi.

A lower limit equation was constructed to represent at least 95 percent confidence that at least 95 percent of all future observations will lie above the lower bound for all data between the lowest and highest stress ranges tested. Details of this calculation procedure are found in Appendix A. Extrapolation of the current data is considered reasonable because the correlation coefficient is very good, and the standard error of the estimate is reasonable. As is common in the fatigue literature, the intercept was adjusted while the slope was held constant [Ref. 6]. In other words, the entire curve was shifted downward. The 95 percent confidence/95 percent probability equations are:

$$S = 311 [N]^{-0.2772} \quad \text{or} \quad (5a)$$

$$N = 9.83 \times 10^8 [S]^{-3.608} \quad (5b)$$

The mean and 95 percent confidence/95 percent probability regression lines are shown in Figure 10. The mean fatigue strength at two million cycles is 12.9 ksi (89 MPa). The fatigue strength at two million cycles using the 95/95 lower bound is 5.6 ksi (39 MPa). The mean fatigue strength at ten million cycles is 8.2 ksi (57 MPa), and the fatigue strength at ten million cycles for at least 95 percent confidence/95 percent probability is 3.6 ksi (25 MPa).

The data collected in the current study were compared to the data published by Archer and Gurney. The fatigue strength at two million cycles predicted for the welds in this study by the mean regression equation is 12.9 ksi (89 MPa), while the data of Archer and Gurney averaged 13.6 ksi (94 MPa) for the two details tested. There is close agreement, approximately 5 percent difference, in mean fatigue strength at two million cycles between the two studies.

The estimate at ten million cycles is not as close; 9.8 ksi (68 MPa) versus Archer and Gurney's average of 6.3 ksi (43 MPa).

The close resemblance of the specimens tested in the current study to the Type S specimens used by Archer and Gurney (e.g. fit-up tolerance and lack of tube-to-plate bearing contact) justifies their combination to create a larger data set. The combined data are shown in Figure 11. This combination of data results in a mean regression equation of:

$$S = 869 [N]^{-0.292} \quad \text{or} \quad (6a)$$

$$N = 1.16 \times 10^{10} [S]^{-3.431} \quad (r^2 = 0.81, \text{SEE} = 1.76) \quad (6b)$$

Where S is in ksi. This is a good curve fit that produces fatigue strength estimates at two and ten million cycles of 12.5 and 7.8 ksi (86 and 54 MPa), respectively.

Calculation of 95 percent confidence/95 percent probability limits for the combined data set results in the following equations:

$$S = 409 [N]^{-0.292} \quad \text{or} \quad (7a)$$

$$N = 8.79 \times 10^8 [S]^{-3.431} \quad (7b)$$

The combined data set with 95 percent confidence/95 percent probability limits estimates fatigue strengths of 5.9 and 3.7 ksi (41 and 26 MPa) at two million and ten million cycles, respectively. Figure 11 shows the 95 percent confidence/95 percent probability line for the combined data set. Comparison of the 95/95 limit equations for the new data and the combined data set shows very good agreement in fatigue strength at both two and ten million cycles. In fact, with rounding, the output of the two equations is equivalent at two million and ten million cycles.

The discussion so far has focused mainly on comparisons of estimated fatigue strengths. Such a comparison is useful for a fatigue design method that uses only fatigue strength as a consideration. The predicted fatigue strengths given by Equation 7a are useful for that purpose. Unfortunately, the usefulness of such a design method is limited when the actual stresses applied are variable, as is the case with wind-loaded sign and signal structures. Regression equations for the fatigue data can estimate the number of fatigue cycles to failure available at a given stress range. One would then be able to quantify fatigue damage. In that context, Equation 7b provides a useful design tool for fatigue life estimation for tube-to-plate fillet welds. One must be careful to note that the fatigue data are only applicable to tube-to-plate fillet welds with loose fit-up clearance and no tube-to-plate bearing contact. This is a very specific, although common, weld connection. Improved fatigue resistance could be expected for tighter fit-up, tube-to-plate bearing contact, or both. The higher reported fatigue strengths for the Type F specimens of Archer and Gurney suggest this improvement.

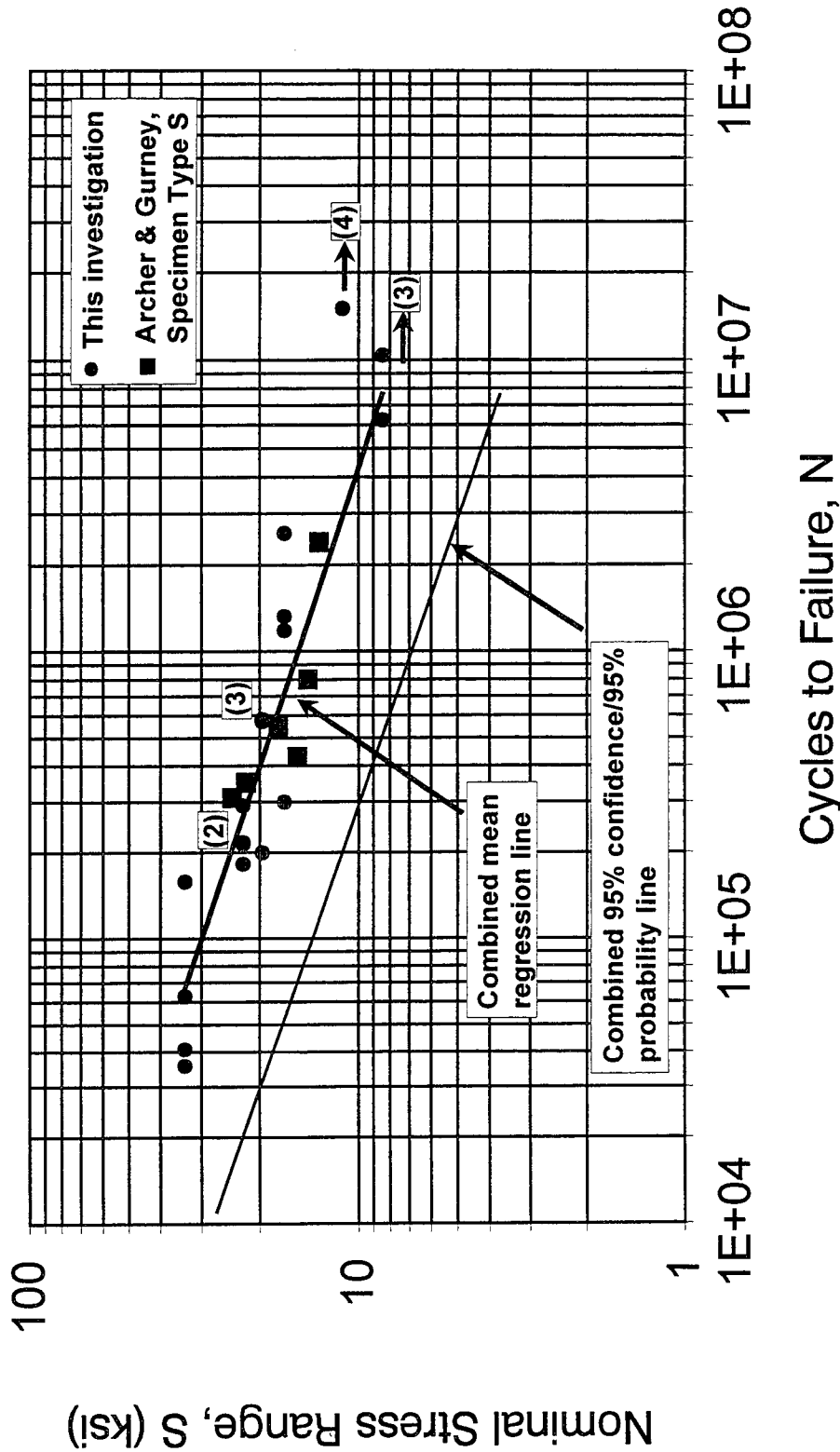


Figure 11. Data from this investigation combined with the Type S specimen data of Archer and Gurney. Combination was based on similarity of fit-up and lack of tube end bearing contact. Arrows indicate tests in the current investigation that were stopped without failure. Numbers in parentheses indicate overlapping data points for the current investigation. The thicker line shows the mean regression line for the combined data equation $S=869[N]^{-0.292}$ with $r^2=0.81$. Mean fatigue strength at 2×10^6 cycles is 12.6 ksi (87 MPa). Mean fatigue strength at 10^7 cycles is 7.9 ksi (26 MPa). The thinner line is the 95% confidence/95% probability equation $S=409[N]^{-0.292}$. With at least 95 percent confidence, one expects at least 95 percent of all future fatigue failures for tube-to-plate welds with similar fit-up tolerances in the as-welded condition to be above this line. Fatigue strengths from the lower bound line are 5.9 ksi (41 MPa) at 2×10^6 cycles and 3.7 ksi (26 MPa) at 10^7 cycles.

The data collected for this study agreed well with Archer and Gurney's published fatigue data regarding the tube-to-plate fillet weld in terms of estimated fatigue strengths at two and ten million cycles. A comparison with existing fatigue limits set by AWS shows that the estimated fatigue strengths are significantly higher than those of a Category ET weld, which is defined as a simple T-, Y-, or K- connection with a partial joint penetration groove weld or fillet weld [Ref. 2, page 165].

The data indicates that the AWS limits established may be overconservative. The combination of IDOT and the specimen Type S data of Archer and Gurney is considered reasonable, because both are tube-to-plate fillet welds with no special fit-up and no tube-to-plate bearing contact. By using either the mean data (Equation 6b), or the 95/95 lower limits (Equation 7b), one is able to estimate the available number of cycles at a given stress range in a fatigue-based design method.

There were not enough specimens tested at very high cycles (10^8) to truly establish an endurance limit. The 95 percent confidence/95 percent probability line may be very conservative at extremely high cycles.

The data presented for the tube-to-plate fillet weld indicate that the AWS Category ET fatigue strengths do not adequately represent this weld joint. Overhead sign and signal structures are almost constantly subjected to various wind loads. The gross number of cycles experienced in service by sign and signal structures will certainly exceed ten million. It is clear that an improvement of the weld joint in terms of fatigue life at all stress ranges is definitely needed.

IV. METHODS TO IMPROVE WELD FATIGUE LIFE

The purpose of this chapter is to discuss various methods to improve the fatigue life of tube-to-fillet welds. Data for methods known to improve fillet welds were extracted from the literature. Fatigue testing of various improvements was beyond the scope of the project.

Background

There are a number of likely sites for initiating fatigue cracks in a welded connection, depending on the nature and orientation of loading with respect to the weld. The most likely failure sites in a properly designed weld are the weld toe or the fillet root. A fillet weld is an abrupt change of section, which introduces a geometric stress concentration. Welds also contain inherent defects, such as lack of fusion, lack of penetration, porosity, or slag inclusions, and are often accompanied by undercut of the weld metal at the toe.

Weld improvement methods usually rely on three principles. The first is to remove the inherent toe defects by improving the local profile. The second is to introduce surface compressive residual stresses at the weld toe to reduce the tensile component of both the residual stress and the applied stress range. Some inherent weld defects can be removed by machining, grinding, or by remelting the weld toe by TIG (tungsten-inert gas) dressing. Surface compressive residual stresses can be introduced by peening.

The third method to improve fatigue resistance of the connection includes weld joint redesign and improved welding practices.

Grinding

Investigations of the effect of grinding the weld toe on weld fatigue strength have been conducted for many years [Ref. 5, Ch.13]. Experimental work on the effect of weld toe grinding is concentrated mainly on AWS Category D and E (plate-type) longitudinal and transverse attachments to load carrying members. Two forms of grinding, disc or burr, are commonly used. From a practical viewpoint, grinding is most widely used at fabrication shops and job sites because of its low cost and cosmetic effect.

Booth [Ref. 7] recommended the depth of grinding be a minimum of 1/32 inch (0.8 mm) beneath the plate surface, with a maximum allowable grinding depth of 5/64 inch (2.0 mm) or five percent of the plate thickness, whichever is greater. The minimum depth was selected to provide adequate removal of weld toe inclusions and undercut. The recommended methods for disc and burr grinding are shown in Figure 17. Recommended equipment for disc grinding

included a hand-held disc grinder (4000 to 8000 rpm) and 35-45 grit grinding discs, either 4 or 7 inch (100 or 175 mm) in diameter. Equipment for burr grinding included a high speed rotary air tool, 15,000 to 20,000 rpm with an oil spray mist unit, 80-100 psi (0.60-0.70 MPa) air supply and tungsten carbide rotary burrs. Proper protective gear is always needed. Severe, deep scratches parallel to the length of the weld are not acceptable. Production rates typically ranged between 3 and 6 ft/man-hour (one and two meters per man-hour).

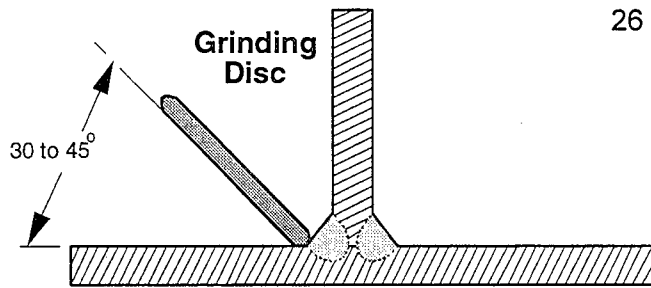
Based on a review of relevant research, Booth noted that weld toe grinding increased fatigue strength at one million cycles by approximately 30 percent. Unfortunately, as pointed out by Booth, the reduction in plate thickness from grinding may become significant in terms of nominal stress levels for relatively thin plates. Booth noted that grinding may not be suitable for joints in plates thinner than approximately 10 mm (0.4 inch). In such cases, Booth recommended considering TIG dressing.

The issue of increased net section stress is important in the case of thin tubes from the viewpoints of increased design dead load stress and the tradeoff between improvement in fatigue resistance and increased applied stress range from the reduction in section. Tube thicknesses used for overhead sign and signal structures are generally less than 5/16 inch (8 mm). A 10 inch (254 mm) nominal diameter tube with wall thickness 0.20 inches (5 mm) would experience approximately a ten percent increase in net section stress for a grinding depth equivalent to five percent of the tube thickness. Very light grinding of the weld toe, say 0.01 inch (0.3 mm) deep, may offer some improvement without a great increase in net section stress. Grinding to improve fatigue resistance should be analyzed carefully before use.

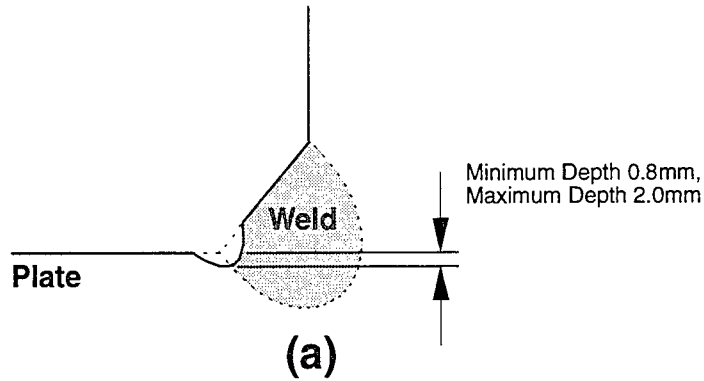
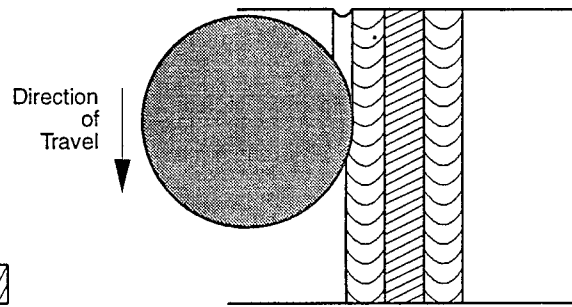
Weld Toe Dressing

Tungsten-inert gas (TIG) dressing involves remelting metal at the weld toe. The purposes of remelting are to improve weld profile by eliminating undercut and to remove inclusions left by the original weld process.

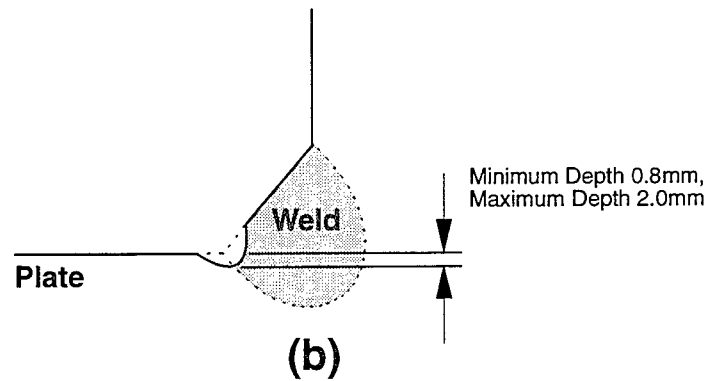
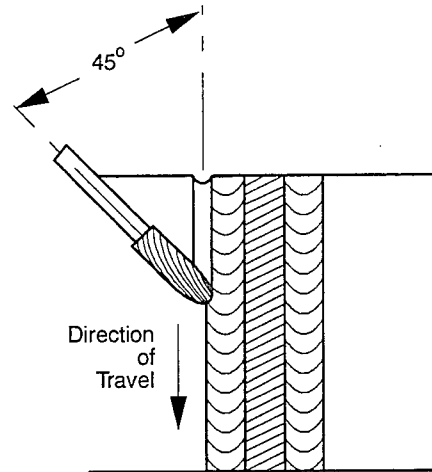
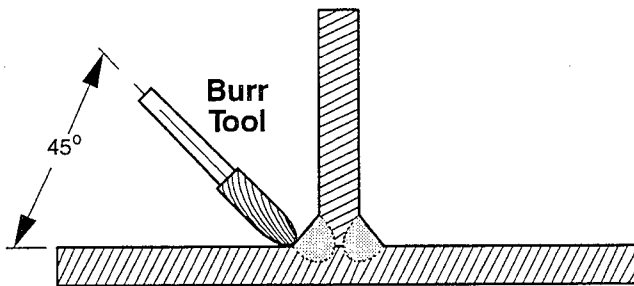
TIG welding became established in industry after World War II, and was mainly used for welding aluminum, austenitic chromium-nickel steels and other non-ferrous metals. TIG welding uses a gas shield composed of argon, helium-argon (typically 75He/25Ar), nitrogen-argon, or pure nitrogen. The most common electrode material is thoriated tungsten which contains 1.5-2.0 percent ThO_2 and operates without melting. Penetration is improved by proper selection of shielding gas and electrode cone angle as noted by Lancaster [Ref. 8, pp. 4-8].



26



(a)



(b)

Figure 13. (a) Recommended method of disc grinding. (b) Recommended method of burr grinding. Recommendations made by Booth [Ref. 7].

Fisher *et al.* [Ref. 9, p. 9] were able to improve penetration by 42 percent using helium-argon shielding and an electrode cone angle of 60 degrees over pure argon shielding for a 200 amp current.

The beneficial effects of TIG dressing have been studied by several investigators [Ref. 5, pp. 306-309]. Reported increases in fatigue strengths generally range between 95 and 250 percent at two million cycles for transverse non-load-carrying fillet welds for plates, although some increases were reported as low as 45 percent. For butt welds, increases were reported to range between 18 and 170 percent, with the majority in the range of 25 to 75 percent. It was noted that TIG dressing was most suited to welds which are transverse to the direction of stress.

For all of the benefits of TIG dressing, there are some disadvantages; the most obvious disadvantages being increased cost and difficulty of proper workmanship. According to Millington [Ref. 10, pp. 134-139], satisfactory TIG beads were difficult to produce unless the surface was clean, preferably lightly ground before weld deposition, and the weld toe wire brushed after dressing to remove contaminants. Adequate heat input was also important (at least 10 kJ/cm, as was keeping the electrode tip sharp [Ref. 5, p.308]. The process was awkward to apply to site conditions because an irregular TIG bead profile was difficult to avoid after accidental stops. A simple method of restarting was found to be reinitiation of the arc about 1/4 inch (6 mm) behind the existing crater. This method was sensitive to operator skill. Another method was to restart the arc on the surface of the weld being treated and then to drop down to the existing crater. When stopping, the arc could be led from the toe to the weld surface [Ref. 5, p.308].

Peening

Peening is a cold-working process by which compressive surface residual stresses are introduced at the weld toe by hitting the surface with either a high velocity stream of hard particles (e.g. metal shot), or with a pneumatic hammer tool. Peening relies on producing plastic surface deformations, which improve fatigue strength from the standpoints of work hardening and compressive residual stress. Peening also produces a (slight) reduction of stress concentration from the improvement of the weld profile.

Two types of hammer peening are commonly available: solid tool and bundled wires or needles. Either type may be operated electrically or by compressed air. Solid tool peening typically uses a 1/2 inch (13 mm) tip diameter. A common wire size used is 1/8 inch (3 mm).

Solid tool peening is usually more effective because greater depth of deformation (thus higher compressive residual stress) can be achieved.

Shot peening frequently uses spherical metal shot, typically 0.02-0.04 inch (0.4-0.9 mm) in diameter, or short pieces of high tensile steel wire which become rounded during use. The effectiveness of shot peening is affected by both shot size and velocity. Typical shot velocity ranges between 150-200 ft/s (45-60 m/s) [Ref. 5, p. 318].

The effect of peening on fatigue strength has been investigated for many years. Published data indicate improvements from as low as 14 percent to as high as 100 percent at two million cycles. Differences documented between solid hammer, multiple wire, and shot peening are shown in Table 5. Solid tool peening resulted in far better improvement than either shot or multiple wire peening.

TABLE 5

Fatigue Strength Improvement of Peened Non-Load-Carrying Fillet Welds

<u>Peening Method</u>	<u>Percent Increase</u>	
	<u>Transverse Welds</u>	<u>Longitudinal Welds</u>
Multiple wire air hammer	20	20
	14	52
Shot peening	36	17
	39	22
Solid tool air hammer	85	90
	100	---

Data Source: Gurney, T. R., *Fatigue of Welded Structures*, Second Edition, Cambridge University Press, London, 1979, p. 320.

Depth of penetration is extremely important. According to Maddox [Ref. 11, pp. 220-224], optimum conditions for hammer peening mild steel fillet welds are those which result in 0.024 inch (0.6 mm) depth of penetration. According to Knight [Ref. 12], four passes of a 1/2 inch (12.5 mm) diameter air hammer operating at approximately 100 psi (0.69 MPa) produced the desired depth of penetration.

It is necessary to make sure that the entire weld toe is properly peened. A major advantage of peening is that inspection requires mainly visual and depth checks. A drawback of peening is that the equipment is heavy and cumbersome. Peening in any position, except

down, is very physically intensive. Also, excessive peening can result in unfavorable conditions, such as cracking or lapping. Noise levels are significant.

Closure

This chapter presented treatment methods to improve the fatigue life of a tube-to-plate fillet weld. Methods discussed included grinding, TIG dressing, and peening. Data for methods known to improve fillet welds were extracted from the literature. Fatigue testing of various improvements was beyond the scope of the project.

It is difficult to recommend a single treatment as the 'best' since each has its own strengths and weaknesses. There may not be a single best weld treatment. In terms of improved fatigue life, TIG dressing offers the best potential improvement. Major drawbacks are cost and difficulty. Grinding has the advantages of ease and low cost, but may not be best for thin tubes because of the reduction in net section and the consequent increase in stress. Peening is also relatively easy and inexpensive, but is prone to cracking or lapping if done in excess.

A combination of grinding and light peening may be good alternative. Shallow grinding followed by shot or hammer peening before galvanizing would help to clean up the weld toe, and provide beneficial compressive surface residual stresses. Galvanizing will affect both the surface compressive residual stresses and the subsurface residual tensile stresses induced by peening.

Another way to improve fatigue performance of the connection is to improve the design. Tighter fit-up tolerances and tube-to-plate bearing contact will provide some improvement. Adequate preheat of the tube and plate will reduce tensile residual stresses by reducing rapid cooling shrinkage stresses on the weld metal. Weld electrodes which better accommodate shrinkage can reduce microcracking at the weld toe.

This report emphasizes improving fatigue performance through treatments in either design or fabrication. Little consideration has been given to repair or retrofit treatments of tube-to-plate fillet welds. Grinding and peening might be appropriate for field work, given adequate controls and inspection. However, there is little room for grinding errors, based on the very shallow depth of grinding recommended; 2 mm maximum or 5 percent of the section, whichever is greater. Field repairs may be expensive, depending on access to each weld connection. Tungsten-inert gas dressing is not recommended for field application given the difficulty of use at fabrication shops. Peening is the most appropriate process for field retrofit. The sheer

number of signal structures in service with these weld connections tends to make general repair or retrofit uneconomical.

The cost and time involved to inspect closely for small cracks in the multitude of overhead sign and signal structures often results in cracks being missed until the member is completely broken. In the case of overhead sign trusses, broken members are often replaced by another welded member. The repair method usually involves lowering the structure to the ground. Immediate replacement of cracked traffic signal structures is usually warranted for safety reasons because cracks tend to grow rapidly under wind loads and many of these structures are nonredundant.

V. SUMMARY

Low fatigue life of tube-to-plate connections is a possible cause of failure in overhead sign and signal structures. This investigation was undertaken because of the effect of structural failures on public safety. The need for this study resulted from (a) reported fatigue failures in Illinois and other states; (b) the lack of sufficient fatigue data specifically for tube-to-plate fillet welds; (c) low published fatigue strengths for the closest geometrically similar AWS fatigue category (Category ET); and (d) the widespread use of tube-to-plate fillet welds in structural details that are susceptible to fatigue damage.

The scope of this report was to (1) investigate the fatigue susceptibility of tube-to-plate fillet welds through literature review and experiment to determine both the fatigue strength of the connection at two million and ten million cycles, and an appropriate equation relating given stress range to expected number of cycles to failure; and (2) examine and discuss possible treatment methods for improving fatigue resistance of the weld.

The fatigue test apparatus and experimental conditions used in this study were described. Tubes fillet welded to a fixed plate were subjected to cantilever bending, with vertical tip deflection of the tube controlled by a slider-crank mechanism. The test apparatus was built to simulate common connections found in cantilever traffic signal structures. Strain was used as the independent variable. Four as-welded specimens were tested at six strain ranges (24 total specimens). The specimens were somewhat smaller than most connections found in service, although the ratio of weld leg to tube thickness was similar. Specimens were tested at three cycles per second. Testing was conducted at the Physical Research Laboratory at Springfield, Illinois. The loading cycle was fully reversed bending with zero mean strain. Cycle data for crack initiation were collected using strain gage instrumentation and a rainflow cycle counting algorithm. The data is reported as nominal stress range versus cycles to crack initiation. Nominal stress range was calculated from $S = E\Delta\epsilon/K_t$ where E is Young's modulus (30×10^6 psi for steel), $\Delta\epsilon$ is the applied strain range measured at the strain gages, and K_t is the stress concentration factor at the strain gage. The stress concentration factor K_t at the location of the strain gage (approximately 3/64 inch away from the weld toe) was found experimentally to be 1.78.

Regression equations were developed for the tube-to-plate fillet weld by combining the new data with the only data found in the literature for a similar weld joint. The regression equations represent at least 95 percent confidence that at least 95 percent of all future observations will lie above the regression line between 8.4 ksi (57.9 MPa) and 33.7 ksi

(232.4 MPa). Extrapolation outside the data range is considered reasonable because the data correlate well and the standard error of the estimate is reasonable. The regression equations (Equations 7a and 7b) are useful for a fatigue design method that incorporates Miner's rule for calculating cumulative fatigue damage.

Test data showed that the as-welded tube-to-plate fillet weld had higher estimated fatigue strengths at both two million and ten million cycles than that published for AWS Category ET welds. The fatigue strength for tube-to-plate fillet welds determined from this study was 5.9 ksi (41 MPa) at two million cycles and 3.7 ksi (26 MPa) at ten million cycles. The fatigue strengths at two million and ten million cycles are useful for design methods that incorporate fatigue strength as a design check. If stresses resulting from expected wind loads exceeded the fatigue strength, the weld joint would need to be redesigned. These wind loads would not be the maximum gust load as defined by current AASHTO design code. A wind loading spectrum would be required.

Grinding, TIG dressing, and peening were examined and discussed as possible methods for improving fatigue resistance of tube-to-plate fillet welds. Each has advantages and disadvantages which result in necessary tradeoffs between effectiveness, cost, difficulty, and possible adverse effects on the weld. The possibilities of either redesign of the weld or improved welding practice were mentioned. The Type F specimens of Archer and Gurney suggest a starting point in terms of fit-up tolerances and tube-to-plate bearing contact. Very light grinding of the weld toe accompanied by full weld peening is a reasonable combination that would offer improvement without a great increase in net section stress. Adequate preheat and low shrinkage electrodes would also help.

VI. CONCLUSIONS AND RECOMMENDATIONS

The following conclusions are made based on the work done during this study:

1. Analysis of the data collected and combined with other published data resulted in a reasonably predictive equation for tube-to-plate fillet welds with loose fit-up and no tube-to-plate bearing contact for expected number of cycles to failure (N) for a given applied stress range (S). The equation for this relationship at the 95% confidence/95% probability level is:

$$N = 8.79 \times 10^8 [S]^{-3.431}$$

where S is in ksi.

2. The estimated fatigue strength at 95% confidence/95% probability of tube-to-plate fillet welds with loose fit-up clearance and no tube-to-plate bearing contact is 5.9 ksi (41 MPa) at two million cycles and 3.7 ksi (26 MPa) at ten million cycles.
3. The regression equations developed in this study are useful for both new design and analysis of existing structures.
4. Although the 95% confidence/95% probability fatigue strengths for the tube-to-plate weld in this study were determined to be higher than those published for AWS Category ET welds, they are low enough to expect fatigue damage in overhead sign and signal structures because of the high number of cycles associated with ambient wind loading. Additional improvement in fatigue resistance is needed for this weld joint.
5. There were not enough tests run at the lower stress ranges to confidently establish a true endurance limit, i.e. a horizontal line on the S-N graph below which failures should not occur. The 95/95 lower limit may be overly conservative beyond fifteen million cycles.
6. The three methods of weld treatment considered in this study are all capable of improving weld joint fatigue strength. Tungsten-inert gas dressing appears to be the most beneficial but is more costly and difficult to accomplish. Grinding offers good improvement and is amenable to both shop and field conditions, but is not recommended for section thicknesses less than about 0.4 inches (10 mm) by Booth [Ref. 7] because of concerns with increasing net section stress at the weld. Peening was the most variable in its effects. Coverage of the area is easy to see visually, but the needed density of coverage is unknown. Too much peening can result in cracking or lapping.

The following recommendations are made:

1. Overhead sign and signal structures should be checked in design for fatigue susceptibility using the 3.7 ksi (26 MPa) fatigue strength determined in this study for ten million cycles. Calculation of wind-induced dynamic stress is needed.
2. If stresses induced by wind loads substantially exceed the fatigue strength, the structure should be analyzed for remaining fatigue life using the N-S equation in an analysis procedure that incorporates a linear cumulative fatigue damage calculation method. One such method is discussed by South [Ref. 1].
3. The weld toe should be lightly ground, about 0.01 inch (0.3 mm) deep and the entire weld should be peened prior to galvanizing.
4. New designs should be introduced and tested. Stress-life equations should be developed for them.
5. Preheat to 200°F minimum of the connection components should be required prior to welding.
6. Future use of tube-to-plate connections should specify tighter fit-up tolerances.
7. Future research should investigate low stress range/very high (100 million) cycles, possible effects of periodic overloads, and low temperature extremes on fatigue behavior.

REFERENCES

1. South, J. M., *Fatigue Analysis of Overhead Sign and Signal Structures*, Physical Research Report 115, Illinois Department of Transportation, 1994.
2. *Structural Welding Code-Steel*, 8th Edition, American Welding Society, Inc., Miami, FL, ANSI/AWS D1.1-84.
3. Hahin, C., South, J. M., Mohammadi, J., Polepeddi, R. K., Accurate and Rapid Determination of Fatigue Damage in Steel Bridges, ASCE, *Journal of Structural Engineering*, Volume 119, Number 1, 1993, pp. 150 - 168.
4. Archer, G. L. and Gurney, T. R. Fatigue Strength of Mild Steel Fillet Welded Tube to Plate Joints, *Metal Construction*, Volume 2, Number 5, 1970, pp. 207-210.
5. Gurney, T. R., *Fatigue of Welded Structures*, Second Edition, Cambridge University Press, London, 1979.
6. Little, R. E., and Jebe, E. H., *Statistical Design of Fatigue Experiments*, Applied Science Publishers, Ltd., London, 1975, Chapter 5.
7. Booth, G. S., Improving the Fatigue Strength of Welded Joints by Grinding-Techniques and Benefits, *Metal Construction*, Volume 18, Number 7, 1986, pp. 432 - 437.
8. Lancaster, J., *Handbook of Structural Welding*, McGraw-Hill, Inc., New York, 1992.
9. Fisher, J., Hausammann, H., Sullivan, M., Pense, A., *Detection and Repair of Fatigue Damage in Welded Highway Bridges*, NCHRP Report 206, Transportation Research Board, Washington, D.C., 1979.
10. Millington, D., TIG Dressing for the Improvement of Fatigue Properties in Welded High Strength Steels, *Metal Construction*, Vol. 5, No. 4, April 1973.
11. Maddox, S. J., Improving the Fatigue Strength of Welded Joints by Peening, *Metal Construction*, Vol. 17, Number 4, 1985.
12. Knight, J. W., *Improving the Fatigue Strength of Fillet Welded Joints by Grinding and Peening*, Welding Institute, Report 8/1976/E.

APPENDIX: DETERMINATION OF CONFIDENCE AND PROBABILITY LIMITS

The following procedure was used to calculate the lower limit line corresponding to at least 95 percent confidence that at least 95 percent of all future observations will lie above the limit line over the entire range of X (stress range). The procedure is also explained by Little and Jebe [Ref. 6]. Data used in this study are included for clarity.

1. Perform a normal linear regression analysis for the available data using $X = \log S$ and $Y = \log N$. Note values of $\sum(x_i)^2$, standard error of Y estimate $S_{Y,X}$ (which is equal to the square root of the variance), and the number of observations n.

Stress Range, S	Cycles to Failure, N	$X = \log S$	$Y = \log N$
33.71	62565	1.5278	4.7963
33.71	157804	1.5278	5.1981
33.71	35629	1.5278	4.5518
33.71	40819	1.5278	4.6109
22.47	216372	1.3516	5.3352
22.47	213422	1.3516	5.3292
22.47	291300	1.3516	5.4643
22.47	182166	1.3516	5.2605
19.63	581212	1.2929	5.7643
19.63	570601	1.2929	5.7563
19.63	199694	1.2929	5.3004
19.63	581206	1.2929	5.7643
16.85	299657	1.2266	5.4766
16.85	2568000	1.2266	6.4096
16.85	1322214	1.2266	6.1213
16.85	1181967	1.2266	6.0726
8.43	6243700	0.9258	6.7954
24.2	309998	1.3838	5.4914
22	350000	1.3424	5.5441
17.6	550000	1.2455	5.7404
15.4	430000	1.1875	5.6335
14.3	800000	1.1553	5.9031
13.2	2400000	1.1206	6.3802

$$\sum(x_i)^2 = 0.45813$$

$$C = 10.06457$$

$$S_{Y,X} = 0.2466$$

$$\text{slope} = -3.431$$

$$n = 23$$

2. Select a range of interest for X such that $X^{**} < X < X^*$. $0.9258 < X < 1.5278$
3. Calculate the mean value of X, designated Xbar. $Xbar = 1.3025$

4. Calculate the following parameters:

$$h = \left[\frac{1}{n} + \frac{(X^{**} - \bar{X})^2}{\sum (x_i)^2} \right]^{1/2} = 0.5942$$

$$g = \left[\frac{1}{n} + \frac{(X^* - \bar{X})^2}{\sum (x_i)^2} \right]^{1/2} = 0.3928$$

$$p = \left[\frac{1}{n} + \frac{(X^{**} - \bar{X})(X^* - \bar{X})}{\sum (x_i)^2} \right] / gh = -0.6073$$

$$A = g/h = 0.6610$$

5. Use $\gamma = 0.02$ for confidence limit (98 percent confidence), $|p|$, and A to look up value of D in tables provided in Reference 6. Interpolate if necessary.

6. Calculate: $C^* = Dg = 3.96 \times 0.3928 = 1.5555$

7. Look up chi-square value for $n-2$ degrees of freedom for $\gamma = 0.02$ (Chi-square = 9.9146). Calculate

$$R = (n-2/\chi^2)^{1/2} = 1.4554$$

8. Look up Z_{2P-1} for a given probability P ($P=0.98$) in a table of standard normal cumulative probabilities ($Z_{2P-1} = 2.0537$). Here, Z_{2P-1} is a standard normal deviate such that a proportion P of the standard normal area is enclosed between $\pm Z_{2P-1}$.

9. The lower limit = $-S_{Y,X} [C^* + R Z_{2P-1}] = -1.12043$

10. The new y-intercept is calculated by subtracting the lower limit from the y-intercept calculated from the regression analysis:

$$b_{\text{new}} = b - \text{lower limit} = 8.94414$$

The antilog of this is the intercept given in Equation 7b ($C = 8.79 \times 10^8$).

11. The confidence and probability statement comes from being able state with at least $[1-\gamma/2-\gamma]100$ percent confidence that a portion $2P-1$ of the populations of interest for $X^{**} < X < X^*$ will exhibit a fatigue strength above the line defined by the new intercept. For this case, $[1-\gamma/2-\gamma]100 = 97$ percent confidence and $2P-1 = 96$ percent. The statement "at least 95 percent confidence and 95 percent probability" is conservative.

